



ELSEVIER

Thermochimica Acta 261 (1995) 183–194

thermochimica  
acta

## Principles for the interpretation of modulated temperature DSC measurements. Part 1. Glass transition

J.E.K. Schawe

*Ifa GmbH, 18 Schillerstrasse, Ulm, D-89077, Germany*

Received 1 July 1994; accepted 17 February 1995

---

### Abstract

A new evaluation method for modulated temperature-DSC measurements based on linear response theory is presented. This yields a complex heat capacity with a real part (storage heat capacity) and an imaginary part (loss heat capacity). This approach makes irreversible (time dependent) thermal events amenable to quantitative and theoretically founded discussion.

This is shown by theoretical analysis and demonstrated experimentally using the glass transition as an example.

*Keywords:* AC calorimetry; DSC; Glass transition; Modulated temperature

---

### List of symbols

$A$	pre-exponential factor of the Arrhenius law
$a_f$	slope of the function $f$
$B$	activation constant of the Arrhenius law
$b_f$	temperature-independent part of the function $f$
$C(t)$	time-dependent heat capacity
$C$	complex heat capacity (Fourier transformational $C(t)$ )
$ C $	modulus of $C$
$C'$	storage heat capacity (real part of $C$ )
$C''$	loss heat capacity (imaginary part of $C$ )
$C^*$	conjugate complex heat capacity
$C_p$	(static) heat capacity of the sample (at constant pressure)
$C_\beta$	time-dependent heat capacity measured at the scanning rate $\beta_0$
$C_\infty$	heat capacity at high frequencies ( $\omega \rightarrow \infty$ )

$f$	time-dependent function, which describes the kinetic component of the measured signal
$f_1$	time-dependent function, which describes the thermodynamic component of the measured signal
$H$	enthalpy
$i$	imaginary unit
$m$	sample mass
$Q$	heat
$q$	specific heat of reaction
$q_{p,T}$	$q$ at constant pressure and temperature
$T$	temperature
$T_a$	temperature amplitude
$T_0$	starting temperature
$t$	time
$t_p$	period of sinusoidal signal

### Greek symbols

$\alpha_\Phi$	linear part of the heat flow of reaction
$\beta$	temperature change
$\beta_0$	scanning rate
$\nu$	rate of reaction
$\nu_{p,T}$	$\nu$ at constant pressure and temperature
$\tau$	relaxation time
$\Phi$	heat flow rate
$\Phi_a$	amplitude of sinusoidal heat flow rate
$\Phi_{dc}$	deconvoluted heat flow rate; underlying heat flow rate
$\Phi_{non}$	“non-reversing” component of heat flow rate
$\Phi_r$	reaction heat flow rate
$\Phi_{rev}$	“reversing” component of heat flow rate
$\varphi$	phase shift between heat flow and temperature
$\psi$	auto-correlation function; retardation function
$\omega$	cyclic frequency
$\omega_0$	cyclic frequency of the measurement
$\omega_\beta$	cyclic frequency of the measured thermal glass transition at the cooling rate $\beta_0$

## 1. Introduction

In handbooks of calorimetry, calorimeters are classified according to their mode of operation. Isothermal, isoperibol, adiabatic and several scanning calorimeters are distinguished [1]. Along with these “classical” methods of calorimetry, so-called AC calorimetry has been used since the sixties [2]. In this method, the reaction of the sample to a sinusoidal temperature change is measured. Along with measurements at

a constant average temperature the periodic temperature change can also be superimposed on a slower linear temperature scan [3]. There are devices described in the literature which function as differential AC-calorimeters [4].

AC-calorimeters are often successfully used in the low temperature range (up to room temperature) [5]. Twin calorimeters are very seldom described.

In an AC-calorimeter the reaction of the sample to a dynamic signal is recorded. In addition to measuring heat capacity [6] and phase transformation [7], relaxation processes have been investigated [8, 9, 10].

Application of the principle of sinusoidal temperature change in a conventional DSC was commercialized some time ago as “Modulated DSC” [11] or “Oscillating DSC” [12]. In these calorimeters, a sinusoidal temperature change is superimposed on the linear scanning program. We suggest calling this measuring method “Modulated Temperature-DSC” (MT-DSC).

With the construction of such calorimeters, the application of this measuring principle for many different materials within a wide temperature range is possible. As a result one can get more information (especially from time-dependent thermal events) than by conventional DSC. However, a problem exists with the current commercial MT-DSC in the evaluation and interpretation of the measured curves.

Typically, the temperature difference  $\Delta T$  between sample and reference is measured. Using a calibration algorithm, the heat flow into the sample  $\Phi(t)$  is calculated from  $\Delta T$ . The calibration procedure is not easy and will be presented elsewhere [13]. If the calibration of the calorimeter is made,  $\Phi(t)$  is assumed to be the true heat flow rate into the sample. This measured (oscillating) heat flow is separated into two parts, the “deconvoluted” heat flow  $\Phi_{dc}$  and the “reversing component”  $\Phi_{rev}$ . The difference between these two is the so-called “non-reversing component”  $\Phi_{non}$ ;  $\Phi_{dc}$  should thus correspond to the conventional DSC signal; and  $\Phi_{rev}$  contains information from processes which are able to follow the alternating heating and cooling. Other processes are reflected in  $\Phi_{non}$  [11].

As a result of our analysis, another method for evaluating MT-DSC measurements will be suggested and discussed using glass transition as an example.

## 2. Theoretical fundamentals

### 2.1. Description of time-dependent linear phenomena

#### 2.1.1. Linear response and heat flow

If a physical system is in equilibrium, then it can be described by time-independent potential functions. Material properties are then described by time-independent parameters (such as dielectric constant, compressibility modulus, and heat capacity). In this case the conventional DSC measurement curves may be described by equilibrium thermodynamics excluding the effects of smearing due to thermal conduction.

However, many thermal events are linked to time-dependent entropy changes, e.g. crystallization and melting of polymers, chemical reactions, biological processes, glass

transition, etc. In conventional DSC a dependence of the measurement curves on the scanning rate may be observed in these cases.

If a thermal event is time dependent, then we can describe this phenomenon with a time-dependent heat capacity  $C(t)$ .  $C(\omega)$  can be obtained from Fourier transformation of  $C(t)$ .

If the disturbances of the system during the measurement are sufficiently small-scale, and the system is close to a local equilibrium, description by means of the linear response theory is possible [14]. This is the simplest theory with which to describe time-dependent phenomena. The glass transition process is a typical example of such a phenomenon [15].

If we change an intensive variable of a system, e.g. the temperature, and we measure an extensive variable, e.g. the enthalpy  $H$ , the relevant material property of the sample is described by the auto-correlation or retardation function  $\psi(t)$ , which characterizes molecular fluctuations. The connection of these quantities is given by the convolution product

$$\partial H(t) = \int_{-\infty}^t \psi(t-t') \partial T(t') dt' \quad (1)$$

This approach to describing time-dependent processes is well known from mechanical and dielectric relaxation investigations [16, 17] and has been used in AC calorimetry evaluation as well [18].

From Eq. (1), the definition of a frequency-dependent complex heat capacity follows [19]

$$C(\omega) = \int_0^{\infty} \psi(t) e^{i\omega t} dt \quad (2)$$

with

$$C(\omega) = C'(\omega) + iC''(\omega) \quad (3)$$

where  $i$  is the imaginary unit.

In the following calculations we use the Fourier transformation method to solve the convolution product. For practical reasons, it is advantageous to introduce the conjugated complex heat capacity as the Fourier transformed  $\psi$ -function

$$C^*(\omega) = \int_0^{\infty} \psi(t) e^{-i\omega t} dt \quad (4)$$

with

$$C^*(\omega) = C'(\omega) - iC''(\omega) \quad (5)$$

This definition of  $C$  shows the connection of the heat capacity with time-dependent molecular movements. The real part of the heat capacity  $C'$  describes molecular motions, and corresponds to  $C_p$  in the case of equilibrium. The imaginary part  $C''$  is linked to dissipation (entropy production [20]). As can be seen, the retardation function  $\psi(t)$  corresponds to the time-dependent heat capacity  $C(t)$ .

In DSC measurements, the heat flow rate

$$\Phi \equiv \left( \frac{dQ}{dt} \right)_p = \frac{dH}{dt} \quad (6)$$

is the measured quantity.

By inserting Eq. (6) into Eq. (1), one obtains the following for the measurement signal

$$\Phi(t) = \int_0^t \psi(t-t') \beta(t') dt' \quad (7)$$

with

$$\beta(t) = \frac{dT}{dt} \quad (8)$$

In the case of a time-independent thermal event, we get from Eqs. (8) and (4)

$$\Phi(t) = C_p \beta(t) \quad (9)$$

This equation is well known in classical DSC.

### 2.1.2. The case of quasi-isothermal conditions

Quasi-isothermal conditions mean that the temperature is altered in a sinusoidal fashion with a frequency  $\omega_0$  and a sufficiently small amplitude  $T_a$  about a constant temperature  $T_0$

$$T(t) = T_0 + T_a \sin(\omega_0 t) \quad (10)$$

For the temperature change  $\beta$ , it follows that

$$\beta(t) = \omega_0 T_a \cos(\omega_0 t) \quad (11)$$

Insertion of Eq. (11) into Eq. (7) yields

$$\Phi(t) = \omega_0 T_a \int_0^t \psi(t-t') \cos(\omega_0 t') dt' \quad (12)$$

After Fourier transformation and insertion of Eq. (4), we obtain from Eq. (12)

$$\Phi(t) = \omega_0 T_a [C'(\omega_0) \cos(\omega_0 t) + C''(\omega_0) \sin(\omega_0 t)] \quad (13)$$

or

$$\Phi(t) = \omega_0 T_a |C(\omega_0)| \cos(\omega_0 t - \varphi) \quad (14)$$

with

$$|C| = \sqrt{C'^2 + C''^2} \quad (15)$$

and

$$C' = |C| \cos \varphi \quad (16a)$$

$$C'' = |C| \sin \varphi \quad (16b)$$

If we define  $\Phi_a$  as the heat flow amplitude of Eq. (14), one obtains the modulus of the complex heat capacity

$$|C(\omega_0)| = \frac{\Phi_a(\omega_0)}{T_a \omega_0} \quad (17)$$

From this value, and the phase shift  $\varphi$  between the heat flow signal and the temperature change, the real and imaginary parts of the heat capacity can be calculated. In general the two components are dependent on the measurement frequency  $\omega_0$ .

Without any thermal event, the static heat capacity  $C_p$  may be determined with the aid of Eq. (17). This method is discussed in Refs. [21, 22].

### 2.1.3. The case of an underlying linear scan

If a sinusoidal change is superimposed on a DSC scan at constant heating rate  $\beta_0$ , the following is valid

$$T(t) = T_0 + \beta_0 t + T_a \sin(\omega_0 t) \quad (18)$$

$$\beta(t) = \beta_0 + \omega_0 T_a \cos(\omega_0 t) \quad (19)$$

According to Eq. (7), the measured heat flow is composed of the superposition of a non-oscillating component on an oscillating one. To determine the phase shift  $\varphi$  and the amplitude  $\Phi_a$  with sufficient accuracy, it is necessary to regard the non-oscillating component as constant during at least one period of the oscillating component. For this reason, thermal events that evolve sufficiently slowly and a low scanning rate are required.

In other words,  $\beta_0$  is sufficiently small if

$$\frac{\beta_0}{\omega_0} \ll 1 \text{ K} \quad (20)$$

Under this condition, one obtains by insertion of Eq. (19) into Eq. (7)

$$\Phi(T(t)) = C_\beta(T)\beta_0 + \omega_0 T_a |C(T, \omega_0)| \cos(\omega_0 t - \varphi) \quad (21)$$

In the case of time-dependent phenomena,  $C_\beta$  corresponds to the apparent heat capacity which, in a conventional DSC measurement, is determined at a heating rate  $\beta_0$  ( $C_\beta$  is different from the thermal event static heat capacity  $C_p$  at equilibrium). For a glass transition, the conventional heating rate  $\beta_0$  can be associated with a certain average frequency  $\omega_\beta$ . Such an effect is observed in the dependence of the glass transition temperature  $T_g$  on the cooling rate [23]. Thus, the following is valid

$$C_\beta(T) \simeq |C(T, \omega_\beta)| \quad (22)$$

The scanning rate for the case considered here is sufficiently small if

$$\omega_\beta \ll \omega_0 \quad (23)$$

Until now it was assumed that the system is in equilibrium. If Eq. (23) is valid, then this condition is fulfilled, at least approximately.

If a pure relaxation process is investigated, we obtain all of the information (the complex heat capacity) from the oscillating component of the heat flow.

In other words, if the experiment is done at a sufficient small underlying scanning rate and an equally small temperature amplitude, then the measured curve is a superposition of two independent signals, an underlying heat flow  $\Phi_{dc}$  (like the conventional DSC signal) and an oscillating heat flow. If the amplitude and phase shift of the oscillating component of heat flow are measured, then the complex heat capacity can be calculated. In the case of time-dependent processes, the heat capacity from the underlying signal  $C_\beta$  and that from the oscillating signal  $|C(\omega_0)|$  are indeed different. Only in the case of measurements without any thermal event are  $C_\beta$  and  $|C(\omega_0)|$  identical.

Another evaluation method is published by Reading and coworkers [11, 24–26]. In this method the oscillating heat flow is separated into a “reversing” and “non-reversing” component. A comparison of this evaluation method with Eq. (21) shows that the “reversing” component is connected to the modulus of the heat capacity  $|C(\omega_0)|$ . The “non-reversing” component results from the difference between  $C_\beta$  and  $|C(\omega_0)|$ . This component is determined by subtracting two curves which were obtained under dissimilar measurement conditions. From the physical point of view the “non-reversing” component does not contain any additional information. A detailed discussion of the differences in the two evaluation methods will be given in Ref. [27].

In the case of phase transitions, the circumstances are quite different and other conditions have to be considered.

## 2.2. The effect of a time-dependent reaction on the heat flow

A detailed discussion of the evaluation of MT-DSC measurements in the presence of time-dependent reactions will be carried out in the second part of this series of articles [28]. However, we regard it necessary to give a brief preview here to show the fundamental consistency of the evaluation methods.

If a time-dependent reaction takes place under isothermal conditions, then on neglecting the entropy variation, the following is valid

$$\Phi_1(t) = \left( \frac{dQ}{dt} \right)_{p,T} = -(mq_{p,T})v_{p,T}(t) \quad (24)$$

where  $(mq_{p,T})$  is the heat of reaction and  $v_{p,T}$  is the rate of reaction [29]. As  $q_{p,T}$  and  $v_{p,T}$  are functions of temperature, it is not correct to use Eq. (24) to evaluate data collected in a scanning mode.

Using the linear approximation and observing the superposition principle, we obtain instead for the corresponding part of the heat flow with temperature change

$$\Phi(T(t)) = \Phi_{T=T_0}(t) - \int_0^t \alpha_\Phi(t-t') \beta(t') dt' \quad (25)$$

with  $\alpha_\Phi$  being the derivative of Eq. (24)

$$\alpha_\Phi(t) = mv(t) \frac{\partial q}{\partial T} + mq \frac{\partial v(t)}{\partial T} \quad (26)$$

If the measurement starts at a sufficiently low temperature, the first term of the summation in Eq. (25) may be left out.

Comparison of Eqs. (7) and (25) shows that the basic approach to evaluate MT-DSC measurements is identical in both cases. However, there are differences in the interpretation.

If the sample is sufficiently far removed from its actual equilibrium, the linear approximation is not valid anymore. It is then possible that no information from the reaction is contained in  $\Phi(t)$ . However, such reactions may be detected in the conventional DSC signal (or the underlying heat flow  $\Phi_{dc}$ ).

### 3. Experimental

We will demonstrate the results of this evaluation method experimentally. The principle of MT-DSC measurements is that a sinusoidal temperature change is superimposed on the normal temperature program. The temperature difference between a furnace with a sample and one with a reference is evaluated. This signal is proportional to the heat flow which is required so that the sample temperature tracks the desired temperature [30]. The proportionality factor (in other words, the calibration function  $K$ ) is dependent on the actual conditions of the heat transfer [31].

Relative to the evaluation method, which is based on the linear response theory, the measured heat flow is divided into three components. First, a separation is made between the non-oscillating and oscillating components by calculation of a sliding average over a period (Eq. (21)). After that, by means of Fourier analysis, the amplitude of the cosine and sine components are determined from the oscillating part of the heat flow (Eq. (13)). From these values,  $C_p$ ,  $C'$  and  $C''$  can then be calculated.

The main problem in a quantitative determination of these parameters is the calibration. The amplitude and phase shift, and consequently the corresponding calibration functions, are determined from the specific thermal conduction conditions in the calorimeter. The calibration functions are dependent on the frequency, the amplitude of the temperature modulation and also on the heat transfer conditions in the sample and calorimeter. Before the measurements were carried out, we worked on the calibration problem. The results, however, will be presented in another paper [13].

All measurements were carried out on a modified Perkin-Elmer DSC 7. In this special calorimeter the program temperature is modulated with a sinusoidal temperature change. The temperature of the sample furnace is also measured. A complete description of this device is in preparation [32]. The influence of heat transfer within the furnaces and of the controllers on the measured signal will also be discussed in that paper. In Refs. [33–36], it is shown that a power compensated DSC is a linear system. All such systems may be used for scanning and modulated measurements. An experimental comparison of heat flux and power compensated DSC in modulated temperature mode is given in Ref. [27].

For the investigations of glass transition behavior we used a certified polystyrene (PS) NIST GM-754.

#### 4. Results

PS ( $m = 17.45$  mg) was cooled from 150 to 70°C with a scanning rate  $\beta_0$  of 1 K min<sup>-1</sup> superimposed by a sinusoidal temperature change with a period  $t_p = 100$  s and an amplitude  $T_a = 1$  K. Fig. 1 shows the complex heat capacity ( $C'$  and  $C''$ ) and  $C_\beta$ . The real part of the heat capacity  $C'$  exhibits a step-shaped change during the glass transition, whereas  $C''$  exhibits a peak. The glass transition observed in  $C_\beta$  occurs at a lower temperature than that for  $C'$ . The transition in  $C_\beta$  is generated by the successive freezing of modes of cooperative molecular motion. The modes which have the greatest actual influence on relaxation behavior at  $\omega_0$  are still not frozen (“in equilibrium”).

As a result of the small value of  $C''$ ,  $C'$  equates with the modulus of the heat capacity  $|C|$ . The difference between the modulus of the complex heat capacity  $|C|$  and  $C_\beta$  results from the different glass transition temperatures, which in turn are a consequence of the different effective measurement frequencies.

The influence of the period  $t_p$  on the measured glass transition is demonstrated in Fig. 2. The glass transition temperature, i.e. the maximum of the  $C''$  peak, increases with decreasing period. The change is 2.6 K per decade: this value

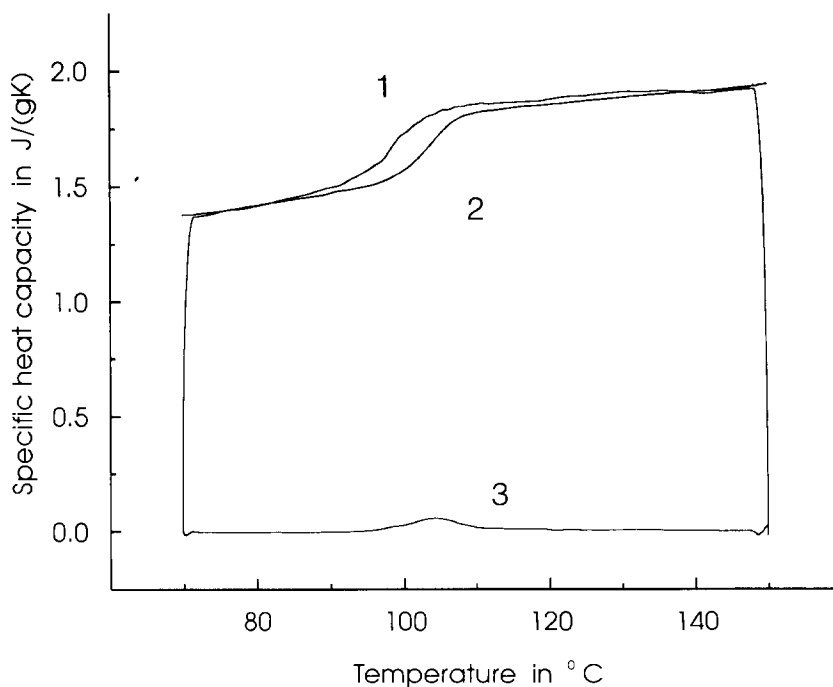


Fig. 1. Glass transition curves of PS analyzed with DSC-measured in the cooling mode ( $\beta_0 = 1$  K min<sup>-1</sup>,  $T_a = 1$  K,  $t_p = 100$  s): 1,  $C_\beta$ ; 2,  $C'$ ; 3,  $C''$ .

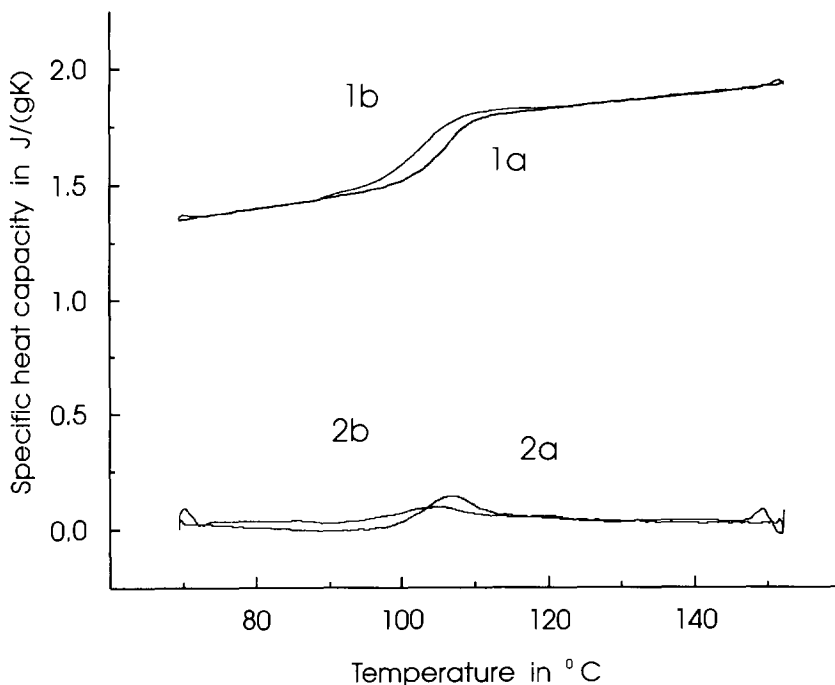


Fig. 2. Glass transition curves of PS analyzed with DSC-measured in the cooling mode with different periods: a,  $\beta_0 = 1 \text{ K min}^{-1}$ ,  $T_a = 1 \text{ K}$ ,  $t_p = 40 \text{ s}$ ; b,  $\beta_0 = 1 \text{ K min}^{-1}$ ,  $T_a = 1 \text{ K}$ ,  $t_p = 200 \text{ s}$ ; 1,  $C'$ ; 2,  $C''$ .

corresponds to the slope of the WLF plot, which is known from dynamic experiments [17].

The results from corresponding heating runs are depicted in Fig. 3. In the heating curves, an effect based on enthalpy retardation has to be expected. With conventional DSC measurement, i.e.  $C_p$  measurements, therefore, a peak in the glass transition region is observed. The dynamic measurements, i.e.  $C'$  and  $C''$ , yield sharper transitions in heating than in cooling mode. This is due to the fact that in the heating mode the deviation from equilibrium is larger than in cooling mode. The  $C'$  and  $C''$  curves do not show any enthalpy retardation peak, because the enthalpy retardation is causally coupled to the thermal glass transition ( $C_p$ ).

If we have physical aging of the sample (structure relaxation), then the glass transition temperature (estimated as fictive temperature) decreases. In the heating mode, the change in heat capacity starts relatively late but is faster (entropy retardation). The main part of the cooperative movements is thawing at temperatures well above the fictive temperature. The reason for this is a decreasing step width of  $C'(T)$  with increasing annealing time. The maximum of the  $C''$  peak does not correspond to the glass transition temperature.

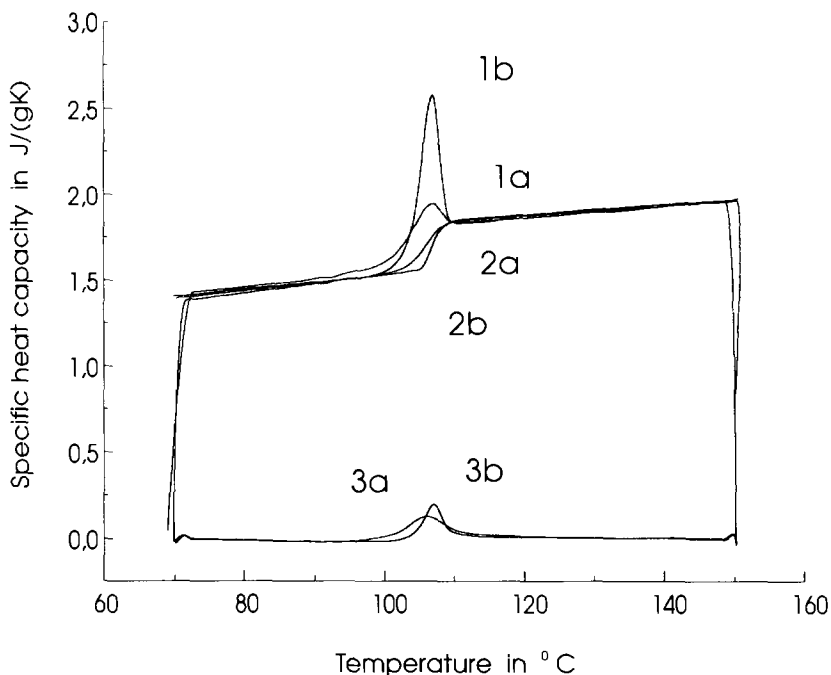


Fig. 3. Glass transition curves of PS analyzed with DSC-measured in the heating mode after cooling with  $2 \text{ K min}^{-1}$ : a,  $\beta_0 = 2 \text{ K min}^{-1}$ ,  $T_a = 1 \text{ K}$ ,  $t_p = 50 \text{ s}$ , without annealing; b,  $\beta_0 = 2 \text{ K min}^{-1}$ ,  $T_a = 1 \text{ K}$ ,  $t_p = 50 \text{ s}$ , after 12 h annealing at  $93^\circ\text{C}$ , 1,  $C_\beta$ ; 2,  $C'$ ; 3,  $C''$ .

## 5. Conclusion

For linear irreversible processes, a method of evaluation has been developed which makes the measurement results amenable to a quantitative assessment. We obtain thereby the heat capacity  $C_\beta(T, \beta)$  which corresponds to the conventional DSC data, as well as the real part  $C'(T, \omega_0)$  and the imaginary part  $C''(T, \omega_0)$  of the heat capacity. These quantities may be used for an exact interpretation on a theoretically correct basis.

## Acknowledgements

The author gratefully acknowledges discussions with Dr. Marcel Margulies and Dr. Bruce Cassel, and the support of the Perkin-Elmer Corporation. Parts of this work were performed in the research and development laboratories of the Perkin-Elmer Corporation in Norwalk, CT.

**References**

- [1] W. Hemminger and G. Höhne, *Calorimetry—Fundamentals and Practice*, Verlag Chemie, Weinheim, 1984.
- [2] P.F. Sullivan and G. Seidel, *Phys. Rev.*, 173 (1968) 679.
- [3] M. Meichle and C.W. Garland, *Phys. Rev. A*, 27 (1983) 2624.
- [4] G.S. Dixon, S.G. Black, C.T. Butler and A.K. Jain, *Anal. Biochem.* 121 (1981) 55.
- [5] G. Bednarz, D.J.W. Geldart and M.A. White, *Phys. Rev. B*, 47 (1993) 14247.
- [6] M. Barrio, J. Font, J. Muntasell and J.L. Tamarit, *J. Therm. Anal.*, 37 (1991) 39.
- [7] C.W. Garland, *Thermochim. Acta*, 88 (1985) 127.
- [8] N.O. Brige and S.R. Nagel, *Phys. Rev. Lett.*, 54 (1985) 2674.
- [9] N.O. Brige, *Phys. Rev. B*, 34 (1986) 1631.
- [10] E. Freire, W.W. van Osdol, O.L. Mayorga and J.M. Sanchez-Ruiz, *Annu. Rev. Biophys. Chem.*, 19 (1990) 159.
- [11] P.S. Gill, S.R. Sauerbrunn and M. Reading, *J. Therm. Anal.*, 40 (1993) 931.
- [12] W.J. Sichina and N. Nakamura, *Oscillating Differential Scanning Calorimetry Software*, Seiko Instr. Product Detail 5.
- [13] J.E.K. Schawe and M. Margulies, in preparation.
- [14] R. Kubo, *Rep. Prog. Phys.*, 29 (1966) 255.
- [15] E. Donth, *Relaxation and Thermodynamics in Polymers*, Akademie-Verlag, Berlin, 1992.
- [16] J.D. Ferry, *Viscoelastic Properties of Polymers*, John Wiley & Sons, London, 1980.
- [17] N.G. McCrum, B.E. Read and G. Williams, *Anelastic and Dielectric Effects in Polymers Solids*, John Wiley & Sons, London, 1970.
- [18] D.H. Jung, T.W. Kwon, D.J. Bae, I.K. Moon and Y.H. Jeong, *Meas. Sci. Technol.*, 3 (1992) 475.
- [19] L.D. Landau and E.M. Lifschitz, *Lehrbuch der Theoretischen Physik*, Bd. V, *Statistische Physik*, Teil 1, Akademie-Verlag, Berlin, 1979.
- [20] R. Haase, *Thermodynamics of Irreversible Processes*, Dover Publications, New York, 1990.
- [21] B. Wunderlich, Y. Jin and A. Boller, *Thermochim. Acta*, 238 (1994) 277.
- [22] A. Boller, Y. Jin and B. Wunderlich, *J. Therm. Anal.*, 42 (1994) 307.
- [23] E. Donth, *J. Non-Cryst. Solids*, 53 (1982) 325.
- [24] M. Reading, D. Elliott and V.L. Hill, *J. Therm. Anal.*, 40 (1993) 941.
- [25] M. Reading, *Trends Polym. Sci.*, 1 (1993) 248.
- [26] M. Reading, A. Luget and R. Wilson, *Thermochim. Acta*, 238 (1994) 295.
- [27] J.E.K. Schawe, *Thermochim. Acta*, in press.
- [28] J.E.K. Schawe, in preparation.
- [29] I. Prigogine, *Thermodynamics of Irreversible Processes*, Interscience Publishers, New York, 1961.
- [30] M.J. O'Neill, *Anal. Chem.*, 36 (1964) 1238.
- [31] G.W.H. Höhne, *Thermochim. Acta*, 69 (1983) 175.
- [32] J.E.K. Schawe et al., in preparation.
- [33] G.W.H. Höhne and J.E.K. Schawe, *Thermochim. Acta*, 229 (1993) 27.
- [34] J.E.K. Schawe, C. Schick and G.W.H. Höhne, *Thermochim. Acta*, 229 (1993) 37.
- [35] J.E.K. Schawe, C. Schick and G.W.H. Höhne, *Thermochim. Acta*, 244 (1994) 49.
- [36] J.E.K. Schawe, *Thermochim. Acta*, 229 (1993) 69.